Development 133, 2435-2445 (2006) doi:10.1242/dev.02408

Fgf8 is required for anterior heart field development

Roger Ilagan[1,2], Radwan Abu-Issa[1], Doris Brown[3], Yu-Ping Yang[2], Kai Jiao[4], Robert J. Schwartz[5], John Klingensmith[2] and Erik N. Meyers[1,2,*]

In the mouse embryo, the splanchnic mesodermal cells of the anterior heart field (AHF) migrate from the pharynx to contribute to the early myocardium of the outflow tract (OT) and right ventricle (RV). Recent studies have attempted to distinguish the AHF from other precardiac populations, and to determine the genetic and molecular mechanisms that regulate its development. Here, we have used an *Fgf8*^{lacZ} allele to demonstrate that *Fgf8* is expressed within the developing AHF. In addition, we use both a hypomorphic *Fgf8* allele (*Fgf8*^{neo}) and *Cre*-mediated gene ablation to show that *Fgf8* is essential for the survival and proliferation of the AHF. *Nkx2.5*^{Cre} is expressed in the AHF, primary heart tube and pharyngeal endoderm, while *TnT*-Cre is expressed only within the specified heart tube myocardium. Deletion of *Fgf8* by *Nkx2.5*^{Cre} results in a significant loss of the *Nkx2.5*^{Cre} lineage and severe OT and RV truncations by E9.5, while the remaining heart chambers (left ventricle and atria) are grossly normal. These defects result from significant decreases in cell proliferation and aberrant cell death in both the pharyngeal endoderm and splanchnic mesoderm. By contrast, ablation of *Fgf8* in the *TnT*-Cre domain does not result in OT or RV defects, providing strong evidence that *Fgf8* expression is crucial in the pharyngeal endoderm and/or overlying splanchnic mesoderm of the AHF at a stage prior to heart tube elongation. Analysis of downstream signaling components, such as phosphorylated-Erk and *Pea3,* identifies the AHF splanchnic mesoderm itself as a target for Fgf8 signaling.

KEY WORDS: Fgf8, Anterior heart field, Cardiogenesis, Cell survival, Proliferation, *Pea3*, *Bmp4*, Erk, Mouse

INTRODUCTION

Myocardial progenitors are derived from early migratory mesoderm that forms bilateral heart fields. These populations organize and coalesce generating the heart field crescent immediately rostral to the forming anterior intestinal portal in the mouse. Through a combination of proliferation and reorganization of the lateral fields, a subset of these myocardial progenitors form the primary heart tube (reviewed by Abu-Issa et al., 2004; Harvey, 2002). The primary heart tube gives rise to the cardiac inflow tract (atria) and the left ventricle. The remaining chambers of the heart, specifically the cardiac outflow tract (OT) and the right ventricle (RV) are derived from the pharyngeal mesoderm contiguous with the primary heart tube. Recent studies in chick and mouse demonstrate that cells within the developing splanchnic mesoderm (SM), as well as possibly the pharyngeal arch core mesoderm (CM), migrate from the pharynx and contribute to the myocardial wall of the OT and RV during early stages of development (Kelly et al., 2001; Mjaatvedt et al., 2001; Waldo et al., 2001). These myocardial precursors have been defined as the anterior heart field (AHF), which we use to describe specifically the SM and CM that contribute to the myocardium of the OT and RV.

In more recent studies, several transcription factors (*Isl1*, *Tbx1*, *Nkx2.5*, *Foxh1*, *Mef2c*) and extracellular signaling molecules (SHH, FGF10, BMP4) that are expressed within or adjacent to the SM and CM have been functionally implicated in AHF development (Baldini, 2004; Cai et al., 2003; Dodou et al., 2004; Lyons et al., 1995; Hu et al., 2004; Jiao et al., 2003; Kelly et al., 2001; Liu et al., 2004; von Both et al., 2004; Xu et al., 2004) (Washington Smoak et al., 2005). Moreover, extensive genetic analyses have shed some light on the regulatory network that guides its development. For example, *Shh* has been implicated as a regulator of *Tbx1* expression through the *Foxa1*, *Foxc1* and *Foxc2* transcription factors (Yamagishi et al., 2003), and *Tbx1* in turn may regulate *Fgf8* expression (Hu et al., 2004). Interestingly, heterozygosity for *Fgf8* increases the incidence of cardiac defects of *Tbx1*$^{+/-}$ embryos (Hu et al., 2004; Vitelli et al., 2002) and *Fgf8* hypomorphic mutants have OT defects, such as double outlet right ventricle and persistent truncus arteriosus (Abu-Issa et al., 2002; Frank et al., 2002).

Fgf8 is a member of a large gene family encoding extracellular ligands that have a wide range of cellular effects depending on the developmental context. Several studies have indicated that there are at least four non-mutually exclusive roles for *Fgf8* in the development of OT defects. First, there is a primary requirement for *Fgf8* during gastrulation, and loss of *Fgf8* results in failure to form a crescent of heart precursor cells (Sun et al., 1999). Second, *Fgf8* is required for establishing the left-right axis and cardiac looping. Abnormalities in this process may affect OT development (Albertson and Yelick, 2005; Meyers and Martin, 1999). Third, *Fgf8* is required for migratory cardiac neural crest cell survival, and therefore OT septation defects could arise from neural crest cell deficiencies (Abu-Issa et al., 2002; Macatee et al., 2003). Finally, *Fgf8* is expressed in the precardiac SM as early as E7.75 (Crossley and Martin, 1995; Kelly et al., 2001) and could have a direct role in AHF maintenance and/or specification. Reduction of the AHF population, and subsequent shortening of the OT, could result in OT septation defects. In zebrafish, it has been demonstrated that the loss of *fgf8* results in the severe truncation of the ventricular myocardial segment (Reifers et al., 2000).

In this study, we have used genetic manipulations to distinguish between these possibilities to better understand how *Fgf8* regulates OT development. We find that *Fgf8* is required for AHF proliferation and survival; furthermore, we define the responsive tissues as well as the expression domains of *Fgf8* that are crucial for AHF development.

[1]Department of Pediatrics, Duke University Medical Center, Durham, NC 27710, USA. [2]Department of Cell Biology, Duke University Medical Center, Durham, NC 27710, USA. [3]Department of Anatomy, School of Medicine, University of California at San Francisco, San Francisco, CA 94143, USA. [4]Department of Genetics, University of Alabama at Birmingham, Birmingham, AL 35294, USA. [5]Institute of Biosciences and Technology, Texas A&M University Health Science Center, Houston, TX 77030, USA.

*Author for correspondence (e-mail: e.meyers@cellbio.duke.edu)

Accepted 18 April 2006

MATERIALS AND METHODS

Mouse lines

All mouse lines used in this study were maintained on mixed genetic backgrounds. Floxed, null and hypomorphic alleles of *Fgf8* (respectively named *Fgf8*^{flox}, *Fgf8*$^{-}$ and *Fgf8*^{neo}) have been previously described (Meyers et al., 1998). The *Fgf8*^{lacZ} 'knock in' line was used to follow *Fgf8* gene expression and was used interchangeably as a null allele (D.B. and G. R. Martin, unpublished). *Nkx2.5*^{Cre} (Moses et al., 2001) and *TnT*-Cre (Jiao et al., 2003) were crossed to the *Cre*-reporter line *Rosa26R* (*R26R*) (Soriano, 1999) to determine the domains of DNA recombination as shown by β-galactosidase (β-gal) activity in the progeny. *Bmp4*^{lacZ} and *Ptch1*^{lacZ} lines have been described previously (Goodrich et al., 1996; Lawson et al., 1999).

Generation of *Cre*-mediated *Fgf8*-null mutants

To generate *Nkx2.5*$^{Cre/+}$; *Fgf8*$^{flox/-}$ embryos, male mice heterozygous for *Nkx2.5*^{Cre} and *Fgf8* were mated to females homozygous for the *Fgf8* floxed allele (*Fgf8*$^{flox/flox}$). The embryos were genotyped for *Cre* and *Fgf8* alleles as previously described (Meyers et al., 1998; Sun et al., 2002). Similar strategies were used to generate *Nkx2.5*$^{Cre/+}$; *Fgf8*$^{flox/lacZ}$ and *TnT*-Cre; *Fgf8*$^{flox/lacZ}$ mutant embryos. For *Cre* lineage trace analysis in the conditional mutant background, *Nkx2.5*$^{Cre/+}$; *Fgf8*$^{+/-}$ males were crossed to females homozygous for both *Fgf8*^{flox} and *R26R*. *Fgf8*^{lacZ}, *Ptch1*^{lacZ} and *Bmp4*^{lacZ} embryos were genotyped for *lacZ* by staining for β-gal activity as described below.

lacZ staining

For embryos containing the *R26R* reporter allele or *Bmp4*^{lacZ}, tissues were fixed for 20 minutes at room temperature in 2% formaldehyde/0.2% glutaraldehyde in PBS with 0.02% NP40, then stained overnight at 37°C in standard X-gal stain. For *Fgf8*^{lacZ} and *Ptch1*^{lacZ} embryos, tissues were fixed for 2-3 minutes at room temperature, followed by standard X-gal stain for 48 to 72 hours at 37°C.

In situ hybridization

Digoxigenin antisense riboprobes were synthesized using template plasmids described in the following: *Fgf8* (Crossley and Martin, 1995), *Wnt11* (Majumdar et al., 2003), *Anf*, *Mhc*, *Mlc2v* (Christoffels et al., 2000) and *Pea3* (Firnberg and Neubuser, 2002). Whole-mount mRNA in situ hybridization was performed essentially as previously described (Neubuser et al., 1997). All results represent at least three mutants and three control embryos.

Immunohistochemistry

All antibodies were diluted in blocking solution containing 3% milk, 0.1% Triton X in PBS. Antibodies were diluted as indicated: phospho-Histone H3 (1:500; Upstate Biotechnology), phospho-Erk (1:200; Cell Signaling Technologies) and AP2α (1:100; Developmental Studies Hybridoma Bank). Alexa Fluor 594 anti-rabbit IgG (Molecular Probes) and Cy2 anti-mouse IgG (Jackson Immuno) secondary antibodies were diluted 1:500. pErk staining was amplified with 1:200 biotinylated anti-rabbit IgG (Vector Laboratories), followed by 1:50 HRP-streptavidin (Jackson Immuno). For peroxidase colorimetric detection, embryos were bleached in 3% H_2O_2 in PBS, and incubated for 10 minutes at room temperature in 0.67 mg/ml 3,3′-diaminobenzidine (DAB, Sigma) in PBS containing 0.1% Tween 20.

Cell death

LysoTracker Red (Molecular Probes) staining has been previously described as a marker for cells death (Zucker et al., 1999). We have performed LysoTracker Red staining as described by Abu-Issa et al. (Abu-Issa et al., 2002), with the exception that DMEM was substituted for Lactated Ringer's Solution.

RESULTS

Fgf8 hypomorphic embryos exhibit cardiovascular and craniofacial defects

Previous analyses of *Fgf8* hypomorphic mutants with variable levels of *Fgf8* expression have revealed a range of cardiovascular phenotypes (Abu-Issa et al., 2002; Frank et al., 2002). Eighty-five percent of *Fgf8*$^{neo/-}$ hypomorphic mutants survive to term with various cardiac defects. Approximately 50% of these embryos have abnormal left-right axis establishment (data not shown), based on earlier ratios of laterality markers as well as organ laterality at term (Meyers and Martin, 1999). The remaining survivors exhibit severe craniofacial and cardiovascular defects, such as double outlet right ventricle (data not shown). These defects are reminiscent of DiGeorge/Velocardiofacial Syndrome and appear statistically and phenotypically independent of left-right defects. Instead, these defects are consistent with significant losses of neural crest cells (Abu-Issa et al., 2002; Macatee et al., 2003) and possibly deficiencies in AHF development.

In order to determine whether defects in the AHF contribute to these observed phenotypes, we examined *Fgf8*$^{neo/-}$ and *Fgf8*$^{neo/lacZ}$ embryos for OT or RV abnormalities at embryonic day (E) 9.5, prior to any substantial contribution of neural crest cell (NCC)-derived populations. Most of the mutant embryos that survive early gastrulation defects exhibit moderate (Fig. 1C) or severe (Fig. 1D) truncations of the OT and RV when compared with stage-matched controls (Fig. 1A). Most of these moderate and severe mutants presumably die by E10.5 owing to circulation failure, as evidenced by pericardial edema (data not shown). The remaining hypomorphic mutants demonstrate mild truncation of the OT/RV (Fig. 1B). These mild *Fgf8*$^{neo/-}$ mutants presumably progress to term with a variety of OT defects such as double outlet right ventricle, which may be the result of the OT/RV hypoplasia. No defects in the atria or left ventricle were evident in our analysis at this stage.

Surprisingly, we noted strong β-gal activity in the developing OT and RV of *Fgf8*$^{+/lacZ}$ embryos at E9.5-E10.5, where *Fgf8* mRNA has not previously been detected. This expression pattern is consistent with a transgenic *Fgf8-lacZ* line which has detectable β-gal activity in the OT (Hu et al., 2004). Given the abnormal OT/RV phenotype and this unexpected expression, we compared the expression of both *Fgf8* mRNA and *Fgf8*^{lacZ} relative to AHF development. *Fgf8*^{lacZ} faithfully recapitulates *Fgf8* mRNA expression pattern in all areas examined between E7.5 and E10.5 with some notable differences described below.

Analysis of *Fgf8* expression relative to heart development

At E7.75, both *Fgf8* mRNA and *Fgf8*^{lacZ} expression are present in bilateral fields immediately caudal to the primary heart field (Crossley and Martin, 1995). These cells ingress inward with the foregut pocket, moving both dorsally and rostrally in relation to the primary heart field. Consistent with this model, both *Fgf8* mRNA and *Fgf8*^{lacZ} are expressed in the SM contiguous with the developing OT between E8.0 and E8.5. (Fig. 2C,C′ and 2D,D′, respectively).

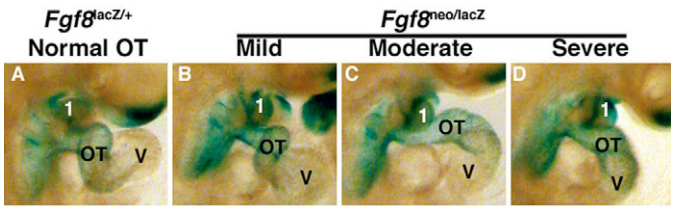

Fig. 1. *Fgf8* hypomorphs have variable length outflow tracts. (**A-D**) *Fgf8*$^{neo/lacZ}$ embryos that undergo relatively normal gastrulation demonstrate OT of variable lengths from mild (B) to moderate and severe (C,D) when compared with control at E9.5 (A). OT, outflow tract; V, ventricle; 1, first pharyngeal arch.

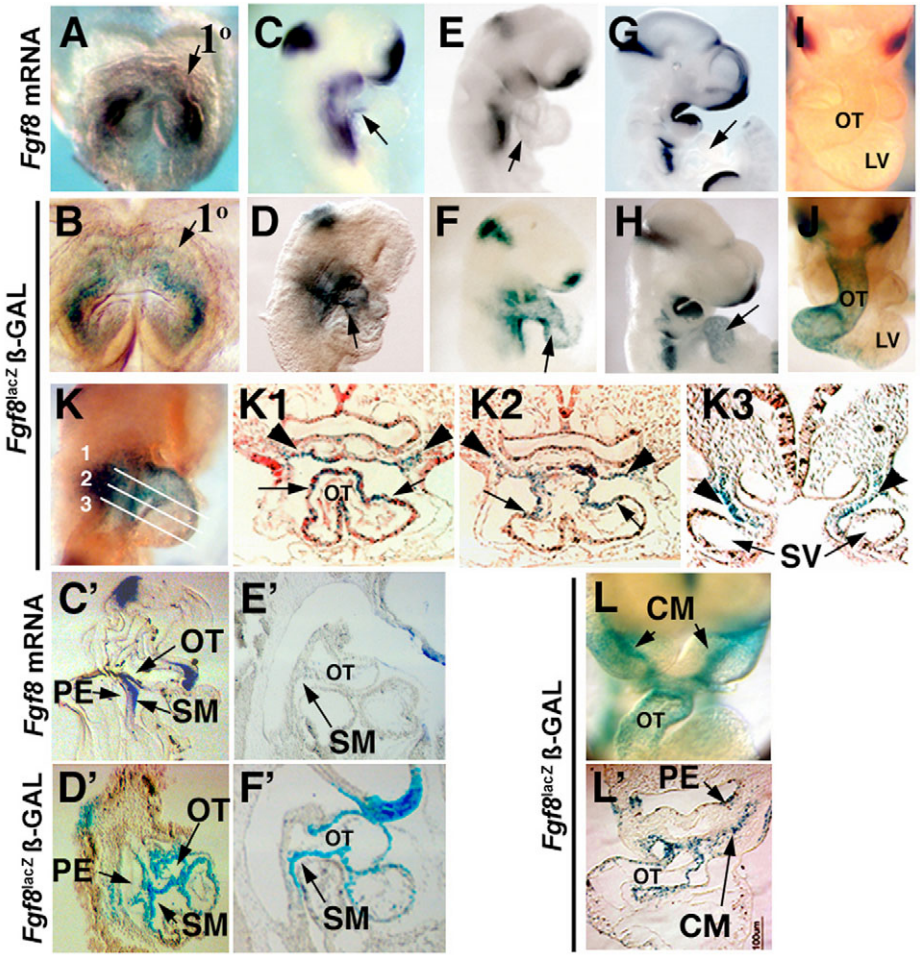

Fig. 2. Comparison of *Fgf8* mRNA expression and *Fgf8*^{lacZ} β-gal activity relative to AHF development. (**A**) *Fgf8* mRNA, as seen by in situ hybridization, is expressed in the presumptive AHF, but not the primary (1°) heart field (arrow) as early as E7.75. (**B**,**D**,**F**,**H**,**J**) *Fgf8*^{lacZ} expression, as seen by β-gal activity, is observed in AHF cells from E7.75 through E10.5 in whole mount. (**C**,**C′**) Expression is later seen in the OT and the contiguous SM at E9.0 in whole-mount (C) and mid-sagittal section (C′). *Fgf8* mRNA levels in the OT and SM become reduced at E9.5 (**E**,**E′**), and is no longer detectable in AHF cells at E10.5 (**G**,**I**). *Fgf8*^{lacZ} expression at E8.5 in whole-mount (**K**) and in transverse sections (**K1-K3**). β-Gal activity is noted in the SM (black arrowheads) and in the outflow tract (OT). Mid-sagittal sections of *Fgf8*^{lacZ} embryos reveal β-gal activity in the PE and SM at E9.0. At E9.5, β-gal activity is noted in the SM and OT (**F′**). At E10.0, *Fgf8*^{lacZ}-positive cells are observed in the pharyngeal CM in whole mount (**L**) and in coronal section (**L′**), which are contiguous with the OT. OT, outflow tract; SM, splanchnic mesoderm; CM, core mesoderm; PE, pharyngeal endoderm; LV, left ventricle; SV, sinus venosus.

Later, between E9.0 and E10.5, *Fgf8* mRNA is expressed in the pharyngeal endoderm and ectoderm in close proximity to the AHF, but not detected in the SM or OT (Fig. 2E,E′,G,I). By contrast, β-gal activity is still detected within the SM and extensively in the OT and RV (Fig. 2F,F′,H). To better define which cells are expressing *lacZ*, we sectioned whole-mount stained embryos at multiple stages. Transverse sections at E8.0 demonstrate expression within the SM extending from the OT myocardium caudally to where the foregut has not closed (Fig. 2K1-K3). In addition, we detect expression at E9.5-E10.0 in the central area of the developing first and second pharyngeal arch, consistent with non-neural crest CM (Fig. 2F,L,L′). These *Fgf8*^{lacZ}-positive CM cells are contiguous with the developing OT wall.

To determine the nature of the discrepancy between *Fgf8* mRNA expression and *Fgf8*^{lacZ} β-gal activity, we analyzed the OT of the heart at E9.5 for *lacZ* mRNA. Although, *lacZ* mRNA was detectable by in situ hybridization in domains of *Fgf8*^{lacZ} β-gal activity (Fig. 3A,B), the mRNA levels appear much lower in proportion to protein activity. Additionally, very low levels (<1% of limb expression) of *Fgf8* message are detected in the OT by RT-PCR (Fig. 3C), which again are out of proportion with β-gal activity. This finding suggests that most of the activity in OT and RV myocardium is the result of residual β-gal protein carried within cells that originated from the AHF external to the developing heart tube, consistent with AHF development models.

Given the expression of *Fgf8*^{lacZ} within the SM and CM, and the cardiac defects associated with *Fgf8* hypomorphic mutants, we hypothesized that *Fgf8* expression is required within the AHF for the development of the OT and RV. To test this hypothesis, we performed genetic ablation of *Fgf8* using the tissue-specific *Cre* lines *Nkx2.5*^{Cre} and *TnT*-Cre.

Nkx2.5^{Cre}, but not *TnT*-Cre, mediates ablation of *Fgf8* in the AHF

The *Nkx2.5* locus targets most cardiogenic populations when expressing *Cre* (Moses et al., 2001; Stanley et al., 2002); however, early cardiac crescent expression of the *Nkx2.5*^{Cre} allele used in this study is somewhat mosaic (data not shown). Nevertheless, complete recombination in the cardiogenic fields is observed at E8.0-E8.5 prior to heart tube elongation (Fig. 4B,B′). Although mesodermal expression of *Fgf8* precedes robust *Nkx2.5*^{Cre} expression, we can use the *Nkx2.5*^{Cre} allele to ablate *Fgf8* in the AHF prior to the elongation process. *Nkx2.5*^{Cre} also targets cells in the heart tube, the ventral pharyngeal endoderm and the anterior ectoderm of the first pharyngeal arch (Fig. 4B,B′,E,E′,E″). As revealed by the *Fgf8*^{lacZ} line, *Fgf8* is expressed in the pharyngeal endoderm, ectoderm, the AHF and the lineage of the AHF (Fig. 4A,A′,D,D′,D″). Therefore, *Fgf8* will functionally be ablated from the AHF, endoderm, first pharyngeal arch ectoderm and subsequent derivatives of these tissues.

By contrast, *TnT*-Cre drives DNA recombination in the primary heart field cardiac crescent as early as E7.5, but not in the AHF precursors (Jiao et al., 2003). Between E8.5 and E11.5, the expression domain is exclusive to the entire myocardium including OT, ventricles and atria. Importantly, *TnT*-Cre is expressed in AHF derivatives only after these cells have migrated into the heart tube proper and differentiated to form the OT and RV myocardium

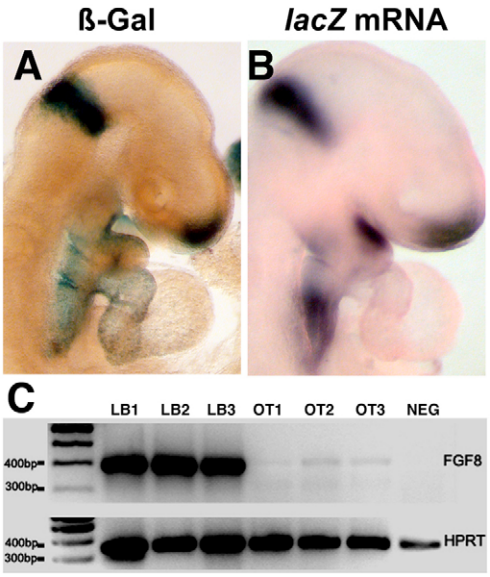

Fig. 3. *Fgf8*^{lacZ} expression reflects endogenous *Fgf8* expression. β-Gal activity in *Fgf8*$^{lacZ/+}$ embryos at E9.5 (**A**) is detected in the OT and RV, and areas of normal *Fgf8* mRNA expression, such as the brain. β-Gal activity correlates with the expression of *lacZ* mRNA seen in whole mount in situ hybridization at E9.5, but very low levels are seen within the OT and RV (**B**). *Fgf8* transcripts are present in the OT at very low levels compared with limb bud controls and HPRT positive controls (**C**) shown by semi-quantitative RT-PCR analysis at E9.5. These data suggest that *Fgf8*^{lacZ} expression accurately reflects *Fgf8* mRNA expression and that β-gal activity is more prominent in OT/RV than either *lacZ* or *Fgf8* mRNA. OT, outflow tract; LB, limb bud; NEG, negative control tissue.

(Fig. 4C,C′,F-F″). *TnT*-Cre is not expressed in the endoderm. Comparisons of both lateral and medial sections of *Fgf8*^{lacZ}, *Nkx2.5*^{Cre}; *R26R* and *TnT*-Cre; *R26R* at E9.5 demonstrate the relevant overlapping domains of expression (Fig. 4D-F,D′-F′,D″-F″).

We defined the regions of functional *Fgf8* deletion by RNA in situ hybridization for the deleted exons of the *Fgf8*^{flox} allele (Fig. 4G-J). We confirmed that *Fgf8* expression is greatly reduced in the AHF of *Nkx2.5*$^{Cre/+}$; *Fgf8*$^{flox/–}$ embryos as early as E8.0 (compare Fig. 4G with 4H) and virtually absent by E9.5 (compare Fig. 4J with 4I), while maintained in other areas of expression such as brain, surface ectoderm and tail bud (where *Nkx2.5*^{Cre} is not expressed). Conversely, *TnT*-Cre recombination resulted in no discernable change in *Fgf8* mRNA expression in the SM or endoderm (data not shown). Phenotypic comparison between *TnT*-Cre; *Fgf8*$^{flox/–}$ embryos and *Nkx2.5*$^{Cre/+}$; *Fgf8*$^{flox/–}$ mutants identify and define the domains of *Fgf8* expression that are necessary for OT and RV development.

Nkx2.5^{Cre}, but not *TnT*-Cre, mediated deletion of *Fgf8* results in OT/RV truncation and pharyngeal arch hypoplasia

We obtained the expected ratio of *Nkx2.5*$^{Cre/+}$; *Fgf8*$^{flox/–}$ class embryos at stages up to E9.5. However, at later time points, we observed a marked reduction in the number of mutant class embryos with no surviving mutants after E10.5. By gross morphology at E9.5, mutant embryos exhibit severely truncated heart tubes and hypoplastic pharyngeal arches (Fig. 5). Using a general marker of specified myocardium (myosin heavy chain, *Mhc*), the left ventricle and both atria appear grossly normal, although slightly dilated, while the presumptive OT and RV are almost completely absent (Fig. 5A,B). Only a small segment of myocardium joins the left ventricle to the aortic sac. To better define the regions of heart tube that are missing, we performed in situ hybridization analysis on the *Nkx2.5*$^{Cre/+}$; *Fgf8*$^{flox/–}$ mutants and littermate controls with a number of regionally specific markers (Fig. 5C-J). *Wnt11*, previously described as a marker specific for the truncus of the OT of the heart (Cai et al., 2003), is completely absent, indicating that mutants are deficient in this region of the OT (Fig. 5C,D). We used the chamber-specific markers atrial natriuretic factor (*Anf*) and myosin light chain 2v (*Mlc2v*) to further characterize the remnant anterior heart segment. *Anf* specifically marks the left ventricle and both atria at E9.5 (Fig. 5E) (Christoffels et al., 2000), while *Mlc2v* is specifically expressed by ventricular myocardium (Fig. 5G) (Cai et al., 2003). We observe in our *Nkx2.5*$^{Cre/+}$; *Fgf8*$^{flox/–}$ mutants that the small anterior heart segment does not express *Anf* (Fig. 5F), but does express *Mlc2v* (Fig. 5H). This analysis suggests that the remnant region is primarily residual right ventricular myocardium, with very little contribution by OT myocardium.

As a final means to characterize the mutant heart tubes, we bred the *Bmp4*^{lacZ} 'knock in' allele onto wild-type and mutant backgrounds, and stained the embryos for β-gal activity. In wild-type controls, *Bmp4*^{lacZ} is expressed in the SM, the OT and at low levels in the RV, but is not expressed in left ventricle or the atria (Fig. 5I) (Jiao et al., 2003). In *Nkx2.5*$^{Cre/+}$; *Fgf8*$^{flox/–}$ mutants, very few *lacZ*-expressing cells are present in the small heart segment, supporting the hypothesis that this region is reduced residual RV (Fig. 5J). The sum of these data indicates that primarily the OT and much of the RV are deficient in these mutant embryos. These are the tissues that derive from the AHF.

Our earlier analysis of both *Fgf8* mRNA and *lacZ* expression reveals low levels in the OT of the heart tube itself. To ascertain any functional role for *Fgf8* expression within the specified myocardium itself rather than the AHF cells, we used the heart tube-specific *TnT*-Cre line. As predicted by our hypothesis, *TnT*-Cre mediated ablation of *Fgf8* does not result in any discernable OT or RV defects when examined at E10.5 (n=15) or OT septation defects at term. In fact, *TnT*-Cre; *Fgf8*$^{flox/–}$ embryos are viable. This finding not only indicates that *Fgf8* expression is dispensable in the myocardium of the differentiated heart tube, but it further suggests that the crucial regions of *Fgf8* expression for heart tube elongation include the AHF and/or the pharyngeal endoderm. These are regions of *Nkx2.5*^{Cre} expression not inclusive of the *TnT*-Cre domain. However, these data do not rule out that OT myocardium could still be responding to FGF8 signals originating from the AHF or pharyngeal endoderm.

The *Nkx2.5*^{Cre} lineage is reduced in the *Nkx2.5*$^{Cre/+}$; *Fgf8*$^{flox/–}$ mutants

As *Nkx2.5*^{Cre} is expressed in the AHF, we can use the *Cre* reporter line *R26R* (Soriano, 1999) to trace the fate of these cells. Using this strategy, we analyzed the *Nkx2.5*^{Cre} lineage in the *Fgf8* conditional mutant background. At stages prior to heart tube elongation (E8.0), we do not observe any change in the number of *R26R lacZ*-expressing cells of *Nkx2.5*$^{Cre/+}$; *Fgf8*$^{flox/–}$; *R26R* mutants. However, differences become noticeable by E8.5-E9.0 as the AHF cells move from the SM and into the heart tube (Fig. 6A,B). By E9.0-E9.5, we observe a significant reduction in β-gal-positive cells in the SM (Fig. 6C-H) and the pharyngeal endoderm (Fig. 6E′,F′), evidenced by the severe thinning of these cell layers (Fig. 6E′,F′). β-gal-positive cells of the CM are also significantly decreased in mutants

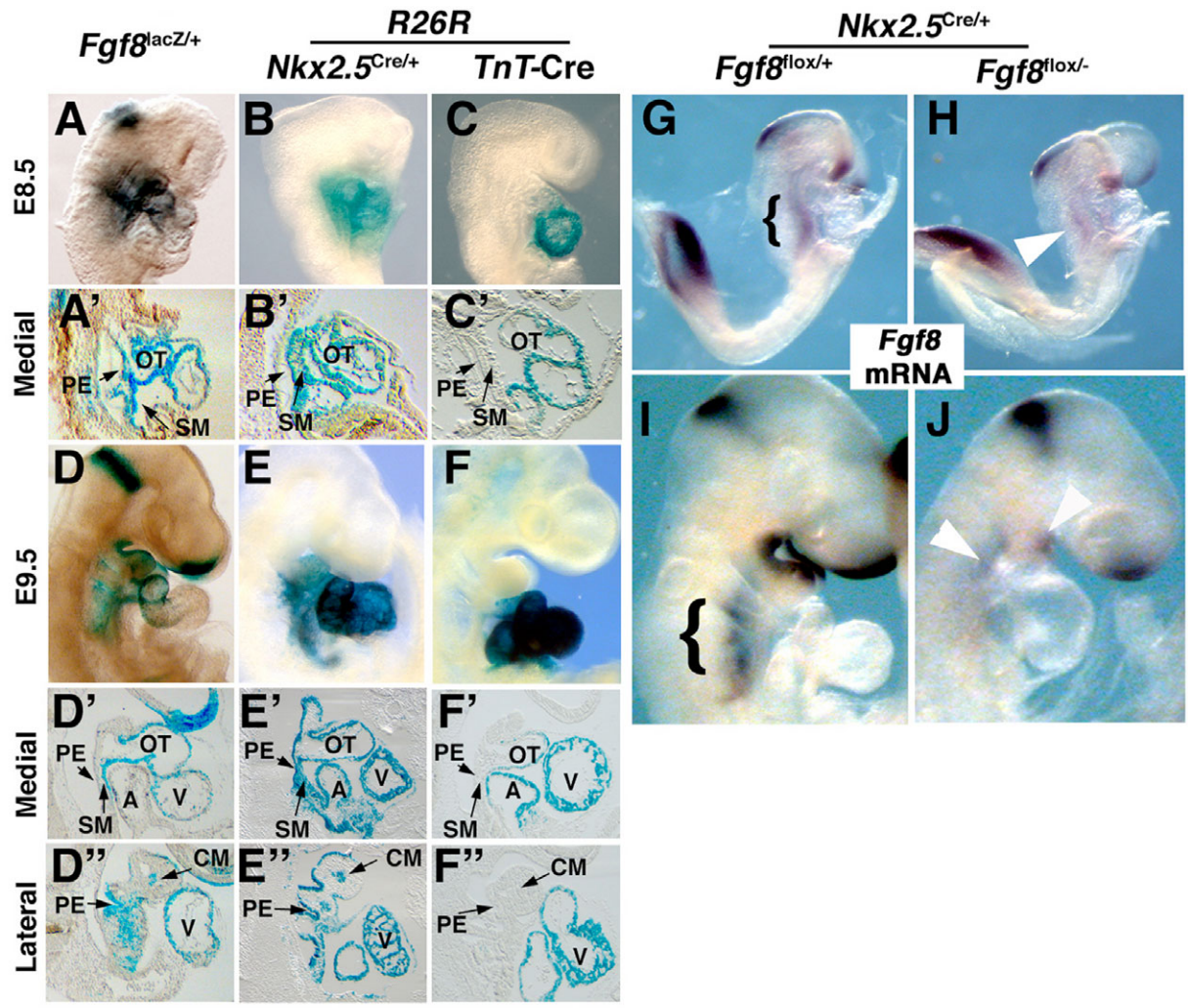

Fig. 4. Tissue-specific ablation studies using *Nkx2.5*^{Cre} and *TnT*-Cre lines. *Fgf8*^{lacZ} expression at E8.5 (**A**,**A′**) overlaps with expression of *Nkx2.5*^{Cre} in the OT, SM and PE (**B**,**B′**). Additionally, *Nkx2.5*^{Cre} and *Fgf8*^{lacZ} expression coincides in the CM at E9.5 (**D-D″** compared with **E-E″**). *TnT*-Cre expression overlaps with *Fgf8*^{lacZ} only in the OT myocardium (**C**,**C′**,**F-F″**). Noted domains of *Nkx2.5*^{Cre} recombination that coincide with *Fgf8*^{lacZ} include the OT, SM, CM and lateral PE, but not surface ectoderm [except for first arch (**D′**,**D″**,**E′**,**E″** and data not shown)]. In situ hybridization analysis for *Fgf8* was performed at E8.5 (**G**,**H**) and E9.5 (**I**,**J**) to confirm genetic ablation in these regions with residual expression in the ectoderm. *Fgf8* mRNA is markedly reduced in the mutants (H,J) compared with normal controls (G,I). OT, outflow tract; SM, splanchnic mesoderm; PE, pharyngeal endoderm; A, atria; V, ventricles.

(Fig. 6G,H). The overall reduction in the *Nkx2.5*^{Cre} lineage strongly suggests that loss of these cells results in the severe heart tube truncation phenotype that is observed in *Fgf8* conditional mutants.

Fgf8^{lacZ} cells are reduced, but not completely absent in mutants

As *Fgf8*^{lacZ} also marks AHF cells, we used the *Fgf8*^{lacZ} allele as a null allele in our ablation scheme to determine the fate of *Fgf8*-expressing cells in *Nkx2.5*$^{Cre/+}$; *Fgf8*$^{lacZ/flox}$ mutant embryos. Phenotypically, *Nkx2.5*$^{Cre/+}$; *Fgf8*$^{flox/lacZ}$ embryos are indistinguishable from *Nkx2.5*$^{Cre/+}$; *Fgf8*$^{flox/-}$ embryos. As seen in whole-mount and section, the overall number of *Fgf8*^{lacZ}-positive cells in the conditional mutants is mildly reduced (Fig. 6J), and, as expected, ectodermal expression remains intact. Again, as seen with the *Nkx2.5*^{Cre} lineage, we observe a loss of AHF cells as shown by the thinning of the SM cell layer (Fig. 6J′). Interestingly, most of the AHF cells that remain in the SM and CM are *Fgf8*^{lacZ} β-gal-positive (Fig. 6J,J′).

We also observe that the OT/RV cells in *Nkx2.5*$^{Cre/+}$; *Fgf8*$^{lacZ/flox}$ mutants are *Fgf8*^{lacZ} positive. Although consistent with our data indicating that this segment is remnant RV, this finding is surprising in that we expected a lineage autonomous function of *Fgf8*, i.e. that deletion of *Fgf8* would result in a loss of all the *Fgf8*^{lacZ}-expressing cells of the heart tube. There are several explanations for the persistence of *Fgf8*^{lacZ}-expressing cells in *Nkx2.5*$^{Cre/+}$; *Fgf8*$^{lacZ/flox}$ embryos. First, this subset of AHF cells may develop independently of *Fgf8*. Second, deletion of *Fgf8* by *Nkx2.5*^{Cre} may not be early enough to affect a small population of AHF as *Fgf8* expression precedes *Nkx2.5* expression. Alternatively, residual RNA or protein after genetic deletion can result in some functional rescue of the earliest AHF cells, which form the RV. The latter two explanations are more likely given that at early stages, *R26R* data clearly demonstrates a relatively normal number of *Nkx2.5*-positive cells of the AHF, and residual *Fgf8* mRNA is observed in mutants (Fig. 4H, Fig. 6B) despite complete recombination between E8.0 and 9.5 (Fig. 4C′,E,E′ and data not shown).

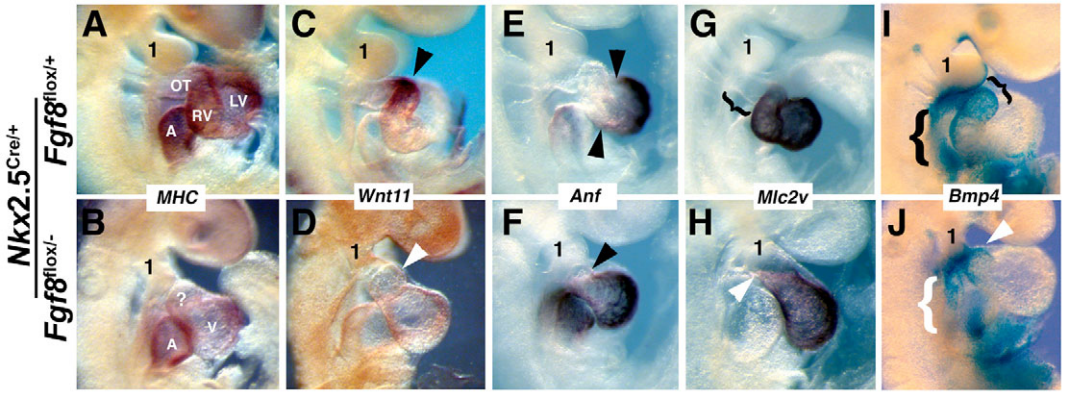

Fig. 5. The anterior heart is truncated in *Nkx2.5*$^{Cre/+}$; *Fgf8*$^{flox/-}$ mutants. Analysis of normal (A,C,E,G,I) and mutant (B,D,F,H,J) embryos at E9.5 was performed by whole mount in situ hybridization (**A-H**) or lacZ stain (**I,J**) for the genes as indicated. *Mhc* is expressed in the myocardium. *Wnt11* is normally expressed in the OT (C, black arrowhead), but is not expressed in mutants (D, white arrowhead). The boundary of *Anf* expression in mutants (E,F, black arrowhead) is in close proximity to the aortic sac, indicating virtual absence of OT/RV. *Mlc2v*-negative myocardium of the proximal OT (G, black bracket) is absent in the mutant (H, white arrowhead). *Bmp4*^{lacZ}-expressing cells are essentially absent in the OT (J, white arrowhead) and splanchnic mesoderm (J, white bracket) compared with normal controls (I, black brackets). 1, first pharyngeal arch; OT, outflow tract; LV, left ventricle; RV, right ventricle; A, atrium.

Erk phosphorylation is reduced in *Nkx2.5*$^{Cre/+}$; *Fgf8*$^{flox/-}$ mutants

FGF8 can function through the receptor tyrosine kinase pathway, leading to the phosphorylation of the MAP kinase Erk (Corson et al., 2003; Katz and McCormick, 1997; Rommel and Hafen, 1998; Sato and Nakamura, 2004). Distribution of phospho-Erk (pErk) can therefore identify tissue targets undergoing active signaling as a result of Fgf8 activity in anterior heart development. We first observe pErk staining in the SM at E8.5 (data not shown). pErk persists until E9.0, where it is observed in the SM as well as the emerging OT, but not significantly in the pharyngeal endoderm (Fig. 7A,A′). After E9.5, when AHF cells have been added and looping is complete, there is an absence in pErk staining in the SM and OT, indicating absence of active signaling through this pathway (data not shown). This decrease in Erk phosphorylation temporally coincides with the observed downregulation of *Fgf8* mRNA, suggesting that Fgf8 signals through Erk in the AHF. If this hypothesis is correct, then loss of *Fgf8* will result in the loss of Erk phosphorylation in the SM. We therefore compared the pErk levels in wild-type and *Nkx2.5*$^{Cre/+}$; *Fgf8*$^{flox/-}$ mutant embryos.

In early cardiac crescent stages, there is no detectable difference in pErk levels between wild-type and mutant embryos (data not shown). This finding is consistent with the fact that at these early stages, *Nkx2.5*^{Cre} expression appears low and incomplete, as revealed by the *R26R* reporter gene. Between E8.5 and E9.5 as the heart tube undergoes elongation, *Nkx2.5*$^{Cre/+}$; *Fgf8*$^{flox/-}$ embryos do not stain positively for pErk in the SM, indicating a loss of signal specifically within these AHF cells (Fig. 7B,B′). It therefore appears that Fgf8 signaling through Erk phosphorylation within the SM is necessary for AHF addition to the myocardium.

Genetic targets *Pea3* and *Bmp4* are reduced in *Nkx2.5*$^{Cre/+}$; *Fgf8*$^{flox/-}$ mutants

To further test our hypothesis that FGF8 signals in an autocrine fashion to the AHF, we analyzed downstream genetic components of the Fgf8 pathway. Members of the ETS family of transcription factors, *Pea3*, *Erm* and *Er81*, are transcriptional targets of FGF8 signaling (Corson et al., 2003; Munchberg and Steinbeisser, 1999; Raible and Brand, 2001; Roehl and Nusslein-Volhard, 2001). *Pea3* is expressed in the SM, the CM and the pharyngeal ecto- and endoderm, suggesting a role for pharyngeal arch and AHF development (Fig. 7C). Genetic ablation of *Fgf8* within the *Nkx2.5*^{Cre} domain results in a significant decrease in *Pea3* expression in the first arch (Fig. 7C,D) as well as undetectable expression within the SM and pharyngeal endoderm (Fig. 7C′,D′). This result provides functional evidence that this *Ets* transcription factor is a downstream target of FGF8 within these tissues. Interestingly, we did not detect expression of activated pErk within the endoderm in wild-type embryos. *Pea3* is expressed in both tissues in wild-type embryos, and is absent in both tissues after *Fgf8* ablation. These data suggest that FGF8 may signal directly to the SM to activate Erk, and that a secondary signal (independent of Erk) may be transduced both in an autocrine fashion to the SM and by a paracrine mechanism to the endoderm to initiate *Pea3* expression. Alternatively, FGF8 could regulate *Pea3* expression independently of Erk activation.

In consideration of the potential crosstalk between the AHF and the pharyngeal endoderm, we determined if *Fgf8* ablation altered other extracellular signaling pathways (*Shh* and *Bmp4*) known to be involved in OT development (Liu et al., 2004) (Washington Smoak et al., 2005). We do not observe any alterations of *Shh* expression in the endoderm of *Nkx2.5*$^{Cre/+}$; *Fgf8*$^{flox/-}$ mutants (Fig. 7G,H). *Ptch1*^{lacZ} expression, which is upregulated in response to activation of the hedgehog pathway (Goodrich et al., 1996), is likewise unaltered in the endoderm and SM (Fig. 7E,E′,F,F′). However, examination of *Bmp4*^{lacZ} expression in the SM of *Nkx2.5*$^{Cre/+}$; *Fgf8*$^{flox/-}$ mutants (Fig. 7I,J and Fig. 5J) indicates a reduction in gene expression. These data reveal that *Fgf8* does not regulate the hedgehog pathway in the SM, but may regulate *Bmp4*. In addition, they suggest that the loss of pErk and *Pea3* expression are indeed the result of *Fgf8* ablation and not the result of dysplastic SM and endoderm, as these tissues are still capable of expressing *Ptch1* and *Shh*, respectively.

Fgf8 is required for proliferation and survival of the precardiac mesoderm and pharyngeal endoderm

Lineage tracing of the *Nkx2.5*^{Cre} domain has revealed a reduction in both the endoderm and SM populations. Therefore, we analyzed cell proliferation in the pharyngeal regions from E8.5 to

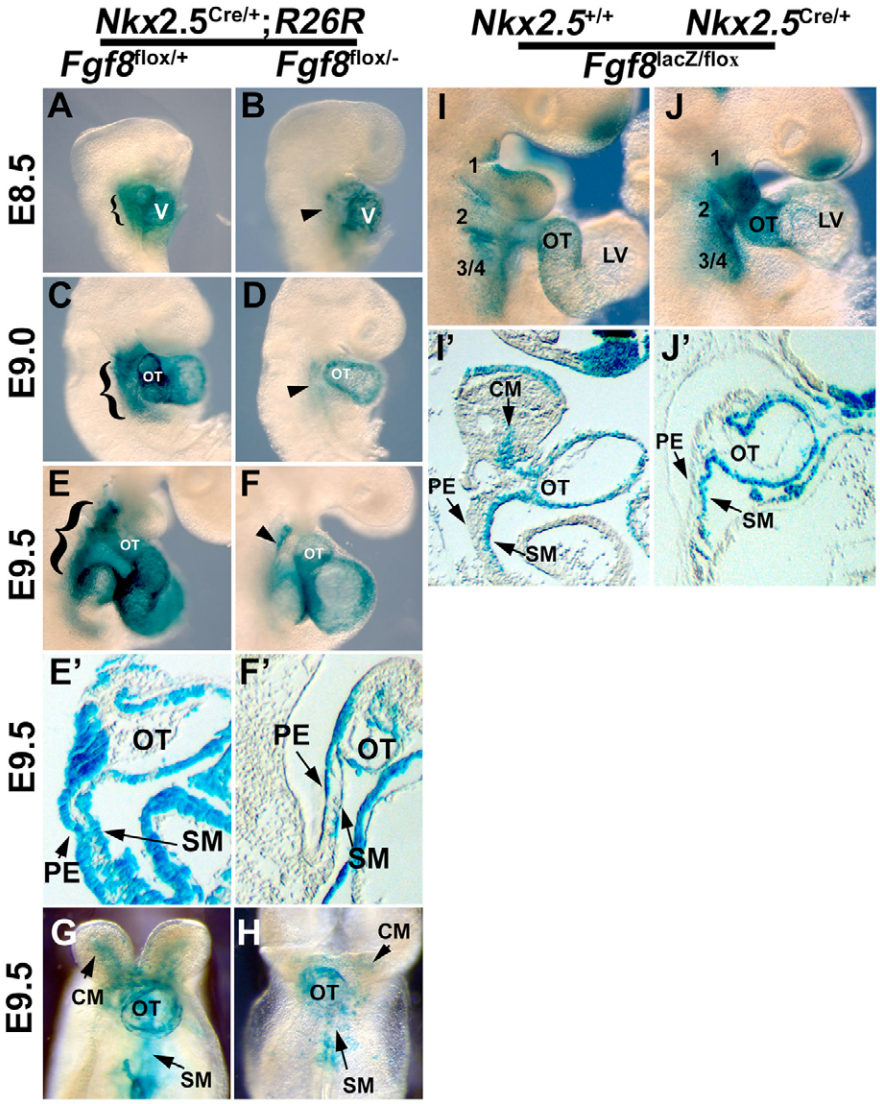

Fig. 6. *Nkx2.5*^{Cre} lineage and *Fgf8*^{lacZ}-expressing cells are reduced in *Nkx2.5*$^{Cre/+}$; *Fgf8*$^{flox/–}$; *R26R* and *Nkx2.5*$^{Cre/+}$; *Fgf8*$^{flox/lacZ}$ mutants, respectively. (**A-F**) Whole-mount *Nkx2.5*^{Cre} lineage analysis from E8.5 to E9.5 indicates a drastic reduction of *lacZ*-positive cells in the mutant class (B,D,F, black arrowheads) when compared with normal controls (A,C,E, black brackets). Histological sections at E9.5 (**E'**,**F'**) reveal a reduction of the *Nkx2.5*^{Cre} lineage in the pharyngeal endoderm (PE) in addition to the splanchnic mesoderm (SM), both of which are thinned with apparent reduced cell number. Ventral views (**G**,**H**) clearly demonstrate the reduction of the *Nkx2.5*^{Cre} lineage in the CM and SM. *Fgf8*^{lacZ}-positive cells are also markedly reduced, but present, in SM and OT in the mutant class at E9.5 (**J**,**J'**) compared with controls (**I**,**I'**). Pharyngeal arches are referred to by their respective numbers (1, 2, 3/4); OT, outflow tract; LV, left ventricle; CM, core mesoderm; V, ventricle.

E9.5 using antibodies for phosphorylated histone H3 (pHH3), which marks mitotic cells. In *Nkx2.5*$^{Cre/+}$; *Fgf8*$^{flox/–}$ mutants, we have observed a significant decrease in cell proliferation in both the SM and pharyngeal endoderm (Fig. 8A,B). A comparison of wild-type and mutant embryos reveals that mitotic indices are reduced by ~50% in the SM and by 60% in the pharyngeal endoderm, although no significant differences in mitotic indices were noted in the outflow region, the left ventricle, atria (Fig. 8G) or the pharyngeal arches (data not shown).

LysoTracker Red analysis from E8.5 to E9.5 reveals that the SM and surrounding tissue undergo excess cell death. Specifically at E9.0, there is an increase in cell death in the SM immediately distal to the emerging OT (Fig. 8C,D), as well as the endoderm adjacent to the SM. By E9.5, once heart tube elongation has been completed, no differences are detected in the SM. However, excess cell death has expanded into the ventral pharyngeal endoderm (data not shown). These data, along with the proliferation studies, reveal that *Fgf8* is necessary for the expansion and maintenance of the precardiac mesoderm, as well as pharyngeal endoderm, and suggest that the truncation of the OT and RV is a result of the reduction in these cell populations.

Neural crest cells undergo excess cell death in *Nkx2.5*$^{Cre/+}$; *Fgf8*$^{flox/–}$ mutants

We and others have previously described abnormal cell death of neural crest cells (NCCs) in *Fgf8* hypomorphs (Abu-Issa et al., 2002; Frank et al., 2002). Interestingly, tissue-specific ablation of *Fgf8* in the *Nkx2.5*^{Cre} domain also results in excess cell death of NCCs in the pharyngeal arch mesenchyme at E9.5 (Fig. 8E,F). The excess cell death in the pharyngeal arch mesenchyme encompasses much of the migratory streams of NCCs up to the dorsal neural tube. These migratory NCCs are specified and migrate in relatively normal streams from the dorsal neural tube as seen by the markers *Ap2α* and *Crabp1* (data not shown). In addition, we see increased cell death of presumptive cardiac NCCs in close proximity to the OT (Fig. 8D).

DISCUSSION

FGF8 signaling to the AHF is required for OT and RV development

In this study, we identify *Fgf8* expression domains that are required for the maintenance and specification of the AHF. Elimination of the *Fgf8* gene specifically from the *Nkx2.5*^{Cre} domain results in aberrant AHF development and ultimately OT/RV truncation. By

contrast, our studies using *TnT*-Cre demonstrate that *Fgf8* expression in the entire primary and AHF-derived myocardium is not crucial. No obvious defects are noted in primary heart field development with either *Nkx2.5* or *TnT*-Cre ablations, suggesting that *Fgf8* expression is not required in these tissues within the time frame of the *Cre* expression. Therefore, *Fgf8* expression must be required in the AHF and/or the pharyngeal endoderm for OT/RV outgrowth and elongation. Interestingly, *Fgf8* ablation in all mesoderm, but not endoderm, can phenocopy *Nkx2.5*$^{Cre/+}$; *Fgf8*$^{flox/–}$ embryos (Park et al., 2006). Although these data suggest that *Fgf8* expression in the SM alone is required for heart tube elongation, this phenotype (driven by *Mesp1*^{Cre}) could represent an earlier defect in mesodermal specification and/or maintenance. Erk phosphorylation is restricted to the SM, and not endoderm, demonstrating that FGF8 signaling to the AHF is crucial for OT/RV outgrowth and development.

Other studies have also used tissue-specific gene deletion to determine the specific functions of the various *Fgf8* expression domains in the pharynx. *Tbx1*-Cre, like *Nkx2.5*^{Cre}, is expressed in both pharyngeal endoderm and mesoderm. *Tbx1*-Cre ablation of *Fgf8* results in DiGeorge-like defects reminiscent of late term *Fgf8* hypomorphs (Brown et al., 2004), but the majority of these mutants do not exhibit the early heart tube truncation phenotype seen in *Nkx2.5*$^{Cre/+}$; *Fgf8*$^{flox/–}$ embryos. As *Nkx2.5*^{Cre} is a null allele, and *Nkx2.5* may lie genetically downstream of *Fgf8* (Alsan and Schulthesis, 2002), *Nkx2.5* heterozygosity may contribute to early OT/RV truncation. However, the *Nkx2.5*$^{Cre/+}$; *Fgf8*$^{flox/–}$ mutants can be phenocopied through the use of other *Cre* lines, such as *Isl1*^{Cre} (Park et al., 2006). Furthermore, we observe the heart tube truncation phenotype in *Fgf8* hypomorphs where *Nkx2.5* gene dose is unaltered.

Phenotypic differences between *Nkx2.5*$^{Cre/+}$; *Fgf8*$^{flox/–}$ embryos and *Tbx1*-Cre; *Fgf8*$^{flox/–}$ embryos may be the result of slightly different *Cre* expression domains. Brown et al. have shown that DNA recombination in the endoderm is complete at E10.5, but the extent of endodermal *Tbx1*-Cre expression at earlier stages may not be complete (C. Brown, personal communication). Incomplete deletion of *Fgf8* in the endoderm earlier in development may explain the discrepancy between *Tbx1*-Cre; *Fgf8*$^{flox/–}$ and *Nkx2.5*$^{Cre/+}$; *Fgf8*$^{flox/–}$ mutants. This explanation suggests a crucial role for early endodermal *Fgf8* expression and AHF expression in the development and outgrowth of the OT/RV. In support of this hypothesis, *Fgf8* ablation specifically in the AHF does not phenocopy the early heart tube truncation phenotype (Park et al., 2006). These data, therefore, suggest a requirement for both domains of *Fgf8* expression for heart tube elongation. Although it remains unclear whether or not endodermal and mesodermal sources of FGF8 have separate and distinct functions, we have nevertheless shown that Fgf8 has a role in determining the length of the OT/RV through proliferation and survival of the AHF.

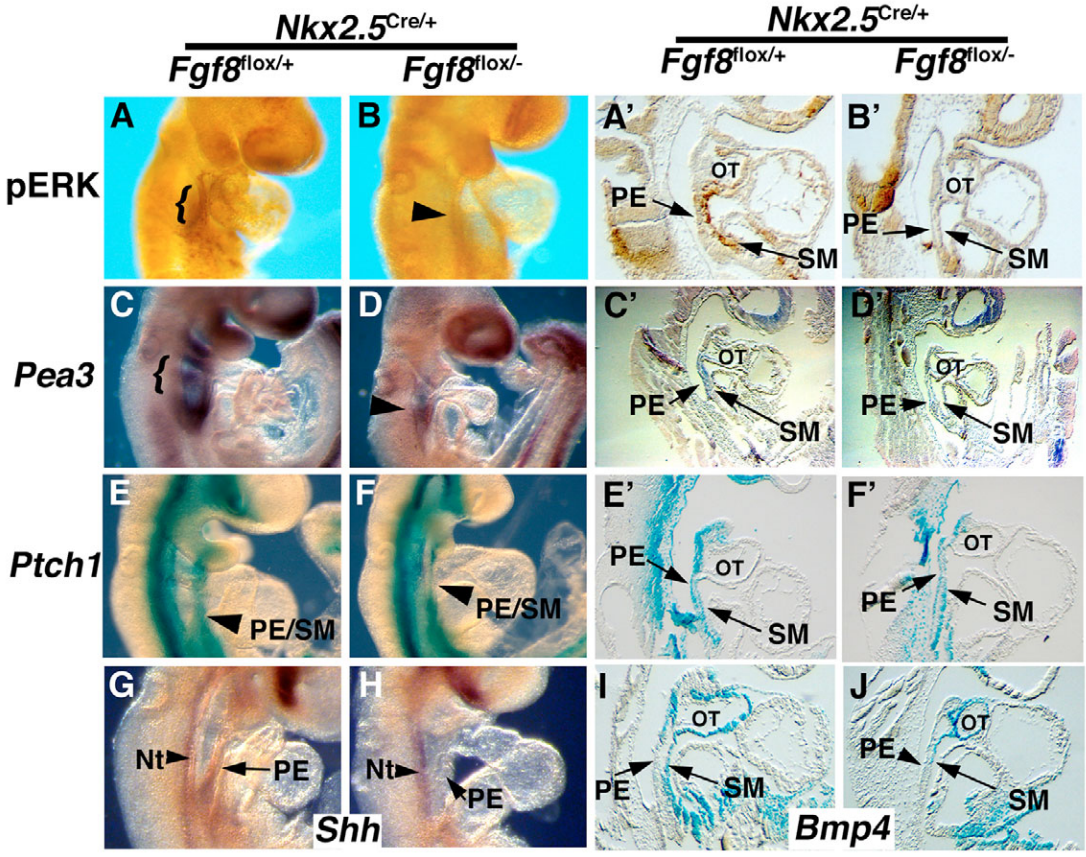

Fig. 7. Cell signaling analysis in *Nkx2.5*$^{Cre/+}$; *Fgf8*$^{flox/–}$ mutants. Immunohistochemistry analysis demonstrates pErk is localized in the SM, but not the PE (**A**,**A′**). *Nkx2.5*^{Cre} elimination of *Fgf8* results in loss of pErk from the SM (**B**,**B′**). RNA in situ hybridization demonstrates that *Pea3* is expressed in the developing arches as well as SM and PE (**C**,**C′**). Loss of *Fgf8* results in continued arch ectoderm expression (**D**, black arrowhead) but loss of SM and PE expression (**D′**). *Ptch1*^{lacZ} β-gal activity (**E-F′**) and *Shh* expression (**G**,**H**) demonstrate that the SM and PE are still capable of *Ptch1* expression, and that *Fgf8* does not regulate this pathway in these tissues. *Bmp4* is downregulated within the SM (**I**,**J**), suggesting a requirement for FGF8 signaling. OT, outflow tract; SM, splanchnic mesoderm; PE, pharyngeal endoderm; Nt, neural tube/notochord.

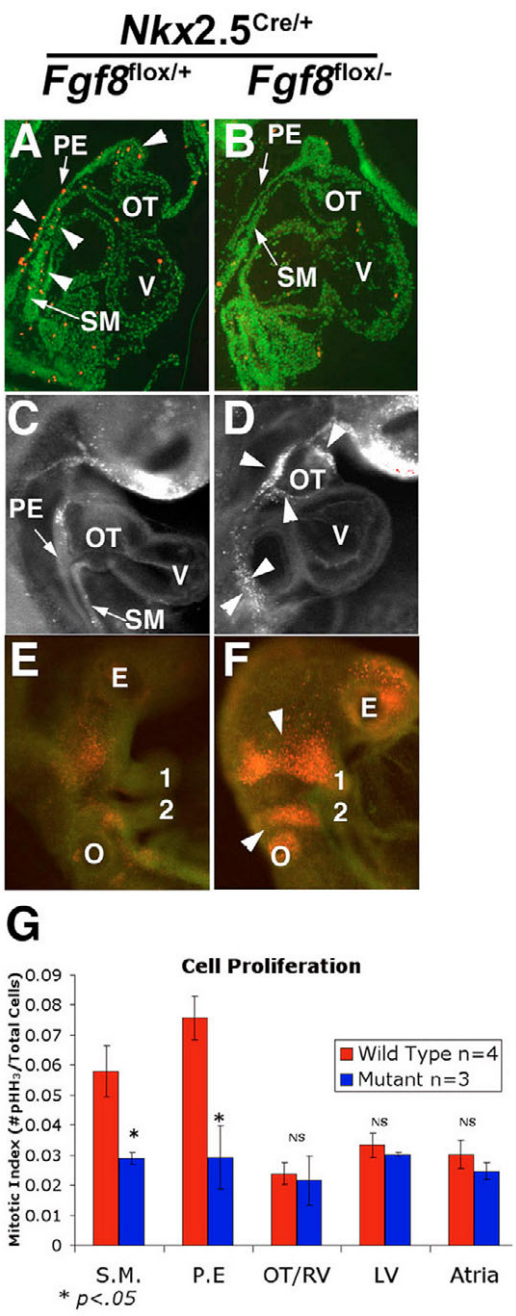

Fig. 8. Cell proliferation and survival are reduced in *Nkx2.5*$^{Cre/+}$; *Fgf8*$^{flox/-}$ mutants. Cell proliferation rates at E9.0 were assessed in section by anti-phospho-histone H3 immunostaining (red) in normal (**A**) and mutant embryos (**B**). SYTO13 counterstain (green) marks nuclei. Marked reduction in proliferation was noted in the PE and SM of mutants compared with controls (n=3 and 4, respectively). Statistical analysis indicates that decreases in cell proliferation in the PE and SM were significant (P<0.05), while rates in the OT, RV, LV and atria were unaltered (**G**). LysoTracker Red staining at E9.0 in normal (**C**) and mutant (**D**) embryos in confocal optical sections (white signal indicates cell death). Increases in cell death are observed in the SM contiguous with the outflow tract (OT) of mutant embryos. Additionally, increases in cell death are observed in the PE at the level of the OT. LysoTracker Red staining at E9.5 (**E**,**F**; red signal indicates cell death) demonstrate that mutant embryos (F) have excess death of NCCs in the pharyngeal arches (1,2). Embryos were counterstained with anti-AP2α (green). OT, outflow tract; SM, splanchnic mesoderm; PE, pharyngeal endoderm; RV, right ventricle; LV, left ventricle; O, otocyst; E, eye.

It is interesting to speculate that the OT septation defects seen in near term *Fgf8* hypomorphic embryos, such as double outlet right ventricle, may reflect alignment defects owing to variable lengthening of the OT. However, it is also possible that alterations in the number or specification of cardiac NCCs entering the OT could also account for such defects. NCCs also have a role in OT elongation as NCC laser ablation results in shortened OT in chick (Farrell et al., 2001; Yelbuz et al., 2002). Distinguishing between such possibilities will be difficult because of potential interactions between the two fields. We are currently investigating the requirement for the Fgf receptor genes *Fgfr1* and *Fgfr2* in the AHF to determine if Fgf signaling has a direct influence on AHF development. Preliminary data indicate that loss of these receptors from the *Nkx2.5*^{Cre} domain results in OT septation defects, but not OT/RV truncation (G. Smyth and E.N.M., unpublished).

Neural crest cells and the anterior heart field

Expansion of the pharyngeal arches is the result of NCCs migrating into the pharyngeal region, forming much of the mesenchyme. Loss of *Fgf8* from the AHF and endoderm results in marked cell death of migratory NCCs (Fig. 8F), similar to that seen in *Fgf8*$^{neo/-}$ embryos (Abu-Issa et al., 2002; Macatee et al., 2003). This expansive cell death can account for the pharyngeal arch hypoplasia observed in *Fgf8* mutants. It was surprising to observe that NCCs located as far as the dorsal neural tube undergo excess cell death in *Nkx2.5*$^{Cre/+}$; *Fgf8*$^{flox/-}$ embryos. This observation leads to two hypotheses. First, given the close apposition and function of the AHF and NCCs in OT development, it is possible that the AHF and NCCs are interdependent. That is, the development of the NCCs depends on signals from the AHF (perhaps through Bmp4). Defective AHF, owing to loss of *Fgf8,* negatively impacts NCC development indirectly. It follows then that pharyngeal arch hypoplasia would result from the loss of NCCs.

The second possibility is that FGF8 protein from the AHF is able to diffuse long distances to directly influence NCC development. However, NCC-specific deletion of both *Fgfr1* and *Fgfr2* does not affect cardiac NCC development, suggesting an indirect effect of FGF8 on these cells in the lower arches (G. Smyth and E. Meyers, unpublished). Alternatively, FGF8 may signal directly to the NCCs through other Fgf receptors.

Role of the pharyngeal arch core mesoderm

Interestingly at E9.5, *Fgf8*^{lacZ} β-gal activity persists within the CM of the pharyngeal arches, but neither *Fgf8* nor *lacZ* mRNA transcripts are detected (data not shown). Previous work has shown that this population of cells is derived from the paraxial mesoderm (Trainor et al., 1994), and *Fgf8* appears to be expressed in this region as early as E8.0 (Crossley and Martin, 1995). The persistence of β-gal activity again could represent a lineage trace of this mesoderm into the core of the pharyngeal arches rather than nascent gene expression.

Gross analyses of the AHF markers *Fgf10*^{lacZ}, *Tbx1*^{lacZ} and *Fgf8*^{lacZ}, as well the *Nkx2.5*^{Cre} lineage trace, reveal that the CM cells are contiguous with the OT (Brown et al., 2004; Kelly et al., 2001). DiI-labeling studies suggest that these CM cells are part of the AHF, and contribute cardiomyocytes to the OT at early stages (Kelly et al., 2001). We have found that like in the SM, there is a marked reduction of the *Nkx2.5*^{Cre}-positive cells in the CM of conditional *Fgf8* mutants. The reduction of CM may not only contribute to OT/RV truncation, but also to pharyngeal arch hypoplasia. Additionally, *Fgf8* expression may be required in the CM for the survival of the NCCs that populate the pharyngeal arches.

At E9.5, when heart tube elongation has been completed, we observe a persistence of *Fgf8*^{lacZ} and *Nkx2.5*^{Cre}-positive cells in the CM. Although these cells remain contiguous with the OT myocardium, it is unlikely that at this stage they continue to contribute to the OT. Instead, these cells are known to give rise to the muscles of the jaw (Trainor et al., 1994). It is intriguing to speculate that OT/RV myocardium and the muscles of the jaw arise from a common lineage represented by the *Fgf8*^{lacZ} allele and *Nkx2.5*^{Cre} line. At the least, the two populations share common genetic regulators required for myogenesis and/or for proper development, such as *Tbx1*, *Isl1* and *Nkx2.5* (Cai et al., 2003; Kelly et al., 2004; Lyons et al., 1995).

Cellular functions of Fgf8 in the anterior heart field

Aside from cell proliferation and survival, FGF8 signaling has a very specific role in gene regulation. FGF8 signaling has been shown to modulate the expression of Wnt (Grieshammer et al., 2005) and Bmp (Lewandoski et al., 2000) genes to pattern the embryo. *Fgf8* has also been shown in vivo to be necessary for expression of various transcription factors such as *Pea3*, *Erm* and *Tbx2* (Firnberg and Neubuser, 2002; Munchberg and Steinbeisser, 1999; Raible and Brand, 2001; Roehl and Nusslein-Volhard, 2001). Here, we have found that *Fgf8* is necessary for *Pea3* expression within the AHF itself, and may also modulate *Bmp4* expression levels.

Many ETS and Fgf proteins have roles in epithelial-to-mesenchymal transition and cell migration (reviewed by Hsu et al., 2004; Thiery, 2002). Fgf1 and Fgf2 have been shown in vitro to induce the internalization and nuclear localization of the cell-adhesion molecule E-cadherin (Bryant et al., 2005). In addition, Fgf signals can activate cell motility through the small GTPase Rho, as seen in *Drosophila* (Schumacher et al., 2004), and through activated Mapk to promote myosin light chain kinase phosphorylation (Klemke et al., 1997). Developmentally, the loss of the Fgf ligand *heartless* in *Drosophila* demonstrates defects in mesodermal migration (Beiman et al., 1996). In mouse, *Fgf8*-null (Sun et al., 1999) and *Fgfr1*-null embryos (Ciruna and Rossant, 2001) have altered cadherin expression, and exhibit migrational defects during gastrulation. We speculate that Fgf8 signaling in the AHF increases cell motility at both the transcriptional and cellular levels, allowing for the migration of cells into the heart tube. Loss of this motility signal may disrupt the AHF program, resulting in increased cell death and decreased proliferation. Studies are currently under way to address this possibility.

The authors thank the following people for probes: B. Hogan (*Pea3*), T. Jessell (*Erm*), G. Martin (*Wnt11*) and A. Moorman (*Anf*, *Mlc2v, Mhc*). We also thank B. Hogan (*Bmp4*^{lacZ}), M. Scott (*Ptch*^{lacZ}) and P. Soriano (*R26R*) for mice. We are grateful to G. Martin for generously providing the *Fgf8*^{lacZ} line prior to publication. We thank Brianne Patton, Danielle Malone and Yin-Xiong Li for technical support. We also thank M. Kirby for many stimulating conversations regarding heart development and for giving us the original idea that *Fgf8* may be involved with AHF development. We thank B. Hogan, M. Kirby and members of the Klingensmith and Meyers laboratories for critical reading of this manuscript. Funding was provided by NIH P01 HL49953 and HL079628 (R.J.S.), HD39948 (E.N.M. and J.K.), DE013674 (J.K.) and R01 HD42803 (E.N.M.).

References

Abu-Issa, R., Smyth, G., Smoak, I., Yamamura, K. and Meyers, E. N. (2002). Fgf8 is required for pharyngeal arch and cardiovascular development in the mouse. *Development* **129**, 4613-4625.

Abu-Issa, R., Waldo, K. and Kirby, M. L. (2004). Heart fields: one, two or more? *Dev. Biol.* **272**, 281-285.

Albertson, R. C. and Yelick, P. C. (2005). Roles for fgf8 signaling in left-right patterning of the visceral organs and craniofacial skeleton. *Dev. Biol.* **283**, 310-321.

Alsan, B. H. and Schultheiss, T. M. (2002). Regulation of avian cardiogenesis by Fgf8 signaling. *Development* **129**, 1935-1943.

Baldini, A. (2004). DiGeorge syndrome: an update. *Curr. Opin. Cardiol.* **19**, 201-204.

Beiman, M., Shilo, B. Z. and Volk, T. (1996). Heartless, a Drosophila FGF receptor homolog, is essential for cell migration and establishment of several mesodermal lineages. *Genes Dev.* **10**, 2993-3002.

Brown, C. B., Wenning, J. M., Lu, M. M., Epstein, D. J., Meyers, E. N. and Epstein, J. A. (2004). Cre-mediated excision of Fgf8 in the Tbx1 expression domain reveals a critical role for Fgf8 in cardiovascular development in the mouse. *Dev. Biol.* **267**, 190-202.

Bryant, D. M., Wylie, F. G. and Stow, J. L. (2005). Regulation of endocytosis, nuclear translocation, and signaling of fibroblast growth factor receptor 1 by E-cadherin. *Mol. Biol. Cell* **16**, 14-23.

Cai, C. L., Liang, X., Shi, Y., Chu, P. H., Pfaff, S. L., Chen, J. and Evans, S. (2003). Isl1 identifies a cardiac progenitor population that proliferates prior to differentiation and contributes a majority of cells to the heart. *Dev. Cell* **5**, 877-889.

Christoffels, V. M., Habets, P. E., Franco, D., Campione, M., de Jong, F., Lamers, W. H., Bao, Z. Z., Palmer, S., Biben, C., Harvey, R. P. et al. (2000). Chamber formation and morphogenesis in the developing mammalian heart. *Dev. Biol.* **223**, 266-278.

Ciruna, B. and Rossant, J. (2001). FGF signaling regulates mesoderm cell fate specification and morphogenetic movement at the primitive streak. *Dev. Cell* **1**, 37-49.

Corson, L. B., Yamanaka, Y., Lai, K. M. and Rossant, J. (2003). Spatial and temporal patterns of ERK signaling during mouse embryogenesis. *Development* **130**, 4527-4537.

Crossley, P. H. and Martin, G. R. (1995). The mouse Fgf8 gene encodes a family of polypeptides and is expressed in regions that direct outgrowth and patterning in the developing embryo. *Development* **121**, 439-451.

Dodou, E., Verzi, M. P., Anderson, J. P., Xu, S. M. and Black, B. L. (2004). Mef2c is a direct transcriptional target of ISL1 and GATA factors in the anterior heart field during mouse embryonic development. *Development* **131**, 3931-3942.

Farrell, M. J., Burch, J. L., Wallis, K., Rowley, L., Kumiski, D., Stadt, H., Godt, R. E., Creazzo, T. L. and Kirby, M. L. (2001). FGF-8 in the ventral pharynx alters development of myocardial calcium transients after neural crest ablation. *J. Clin. Invest.* **107**, 1509-1517.

Firnberg, N. and Neubuser, A. (2002). FGF signaling regulates expression of Tbx2, Erm, Pea3, and Pax3 in the early nasal region. *Dev. Biol.* **247**, 237-250.

Frank, D. U., Fotheringham, L. K., Brewer, J. A., Muglia, L. J., Tristani-Firouzi, M., Capecchi, M. R. and Moon, A. M. (2002). An Fgf8 mouse mutant phenocopies human 22q11 deletion syndrome. *Development* **129**, 4591-4603.

Goodrich, L. V., Johnson, R. L., Milenkovic, L., McMahon, J. A. and Scott, M. P. (1996). Conservation of the hedgehog/patched signaling pathway from flies to mice: induction of a mouse patched gene by Hedgehog. *Genes Dev.* **10**, 301-312.

Grieshammer, U., Cebrian, C., Ilagan, R., Meyers, E., Herzlinger, D. and Martin, G. R. (2005). FGF8 is required for cell survival at distinct stages of nephrogenesis and for regulation of gene expression in nascent nephrons. *Development* **132**, 3847-3857.

Harvey, R. P. (2002). Patterning the vertebrate heart. *Nat. Rev. Genet.* **3**, 544-556.

Hsu, T., Trojanowska, M. and Watson, D. K. (2004). Ets proteins in biological control and cancer. *J. Cell Biochem.* **91**, 896-903.

Hu, T., Yamagishi, H., Maeda, J., McAnally, J., Yamagishi, C. and Srivastava, D. (2004). Tbx1 regulates fibroblast growth factors in the anterior heart field through a reinforcing autoregulatory loop involving forkhead transcription factors. *Development* **131**, 5491-5502.

Jiao, K., Kulessa, H., Tompkins, K., Zhou, Y., Batts, L., Baldwin, H. S. and Hogan, B. L. (2003). An essential role of Bmp4 in the atrioventricular septation of the mouse heart. *Genes Dev.* **17**, 2362-2367.

Katz, M. E. and McCormick, F. (1997). Signal transduction from multiple Ras effectors. *Curr. Opin. Genet. Dev.* **7**, 75-79.

Kelly, R. G., Brown, N. A. and Buckingham, M. E. (2001). The arterial pole of the mouse heart forms from Fgf10-expressing cells in pharyngeal mesoderm. *Dev. Cell* **1**, 435-440.

Kelly, R. G., Jerome-Majewska, L. A. and Papaioannou, V. E. (2004). The del22q11.2 candidate gene Tbx1 regulates branchiometric myogenesis. *Hum. Mol. Genet.* **13**, 2829-2840.

Klemke, R. L., Cai, S., Giannini, A. L., Galllagher, P. J., de Lanerolle, P. and Cheresh, D. A. (1997). Regulation of cell motility by mitogen-activated protein kinase. *J. Cell Biol.* **137**, 481-492.

Lawson, K. A., Dunn, N. R., Roelen, B. A., Zeinstra, L. M., Davis, A. M., Wright, C. V., Korving, J. P. and Hogan, B. L. (1999). Bmp4 is required for the generation of primordial germ cells in the mouse embryo. *Genes Dev.* **13**, 424-36.

Lewandoski, M., Sun, X. and Martin, G. (2000). Fgf8 signalling from the AER is essential for normal limb development. *Nat. Genet.* **26**, 460-463.
Liu, W., Selever, J., Wang, D., Lu, M. F., Moses, K. A., Schwartz, R. J. and Martin, J. F. (2004). Bmp4 signaling is required for outflow-tract septation and branchial-arch artery remodeling. *Proc. Natl. Acad. Sci. USA* **101**, 4489-4494.
Lyons, I., Parsons, L. M., Hartley, L., Li, R., Andrews, J. E., Robb, L. and Harvey, R. P. (1995). Myogenic and morphogenetic defects in the heart tubes of murine embryos lacking the homeo box gene Nkx2-5. *Genes Dev.* **9**, 1654-1666.
Macatee, T. L., Hammond, B. P., Arenkiel, B. R., Francis, L., Frank, D. U. and Moon, A. M. (2003). Ablation of specific expression domains reveals discrete functions of ectoderm- and endoderm-derived FGF8 during cardiovascular and pharyngeal development. *Development* **130**, 6361-6374.
Majumdar, A., Vainio, S., Kispert, A., McMahon, J. and McMahon, A. P. (2003). Wnt11 and Ret/Gdnf pathways cooperate in regulating ureteric branching during metanephric kidney development. *Development* **130**, 3175-3185.
Meyers, E. N. and Martin, G. R. (1999). Differences in left-right axis pathways in mouse and chick: functions of FGF8 and SHH. *Science* **285**, 403-406.
Meyers, E. N., Lewandoski, M. and Martin, G. R. (1998). An Fgf8 mutant allelic series generated by Cre-and Flp-mediated recombination. *Nat. Genet.* **18**, 136-141.
Mjaatvedt, C. H., Nakaoka, T., Moreno-Rodriguez, R., Norris, R. A., Kern, M. J., Eisenberg, C. A., Turner, D. and Markwald, R. R. (2001). The outflow tract of the heart is recruited from a novel heart-forming field. *Dev. Biol.* **238**, 97-109.
Moses, K. A., DeMayo, F., Braun, R. M., Reecy, J. L. and Schwartz, R. J. (2001). Embryonic expression of an Nkx2-5/Cre gene using ROSA26 reporter mice. *Genesis* **31**, 176-180.
Munchberg, S. R. and Steinbeisser, H. (1999). The Xenopus Ets transcription factor XER81 is a target of the FGF signaling pathway. *Mech. Dev.* **80**, 53-65.
Neubuser, A., Peters, H., Balling, R. and Martin, G. R. (1997). Antagonistic interactions between FGF and BMP signaling pathways: a mechanism for positioning the sites of tooth formation. *Cell* **90**, 247-255.
Park, E. J., Ogden, L. A., Talbot, A., Evans, S., Cai, C. L., Black, B., Frank, D. U. and Moon, A. M. (2006). Required, tissue-specific roles for Fgf8 in outflow tract formation and remodeling. *Development* **133**,2419-2433.
Raible, F. and Brand, M. (2001). Tight transcriptional control of the ETS domain factors Erm and Pea3 by Fgf signaling during early zebrafish development. *Mech. Dev.* **107**, 105-117.
Reifers, F., Walsh, E., Leger, S., Stainier, D. and Brand, M. (2000). Induction and differentiation of the zebrafish heart requires fibroblast growth factor 8 (fgf8/acerebellar). *Development* **127**, 225-235.
Roehl, H. and Nusslein-Volhard, C. (2001). Zebrafish pea3 and erm are general targets of FGF8 signaling. *Curr. Biol.* **11**, 503-507.
Rommel, C. and Hafen, E. (1998). Ras – a versatile cellular switch. *Curr. Opin. Genet. Dev.* **8**, 412-418.
Sato, T. and Nakamura, H. (2004). The Fgf8 signal causes cerebellar differentiation by activating the Ras-ERK signaling pathway. *Development* **131**, 4275-4285.
Schumacher, S., Gryzik, T., Tannebaum, S. and Muller, H. A. (2004). The RhoGEF Pebble is required for cell shape changes during cell migration triggered by the Drosophila FGF receptor Heartless. *Development* **131**, 2631-2640.
Soriano, P. (1999). Generalized lacZ expression with the ROSA26 Cre reporter strain. *Nat. Genet.* **21**, 70-71.
Stanley, E. G., Biben, C., Elefanty, A., Barnett, L., Koentgen, F., Robb, L. and Harvey, R. P. (2002). Efficient Cre-mediated deletion in cardiac progenitor cells conferred by a 3′UTR-ires-Cre allele of the homeobox gene Nkx2-5. *Int. J. Dev. Biol.* **46**, 431-439.
Sun, X., Meyers, E. N., Lewandoski, M. and Martin, G. R. (1999). Targeted disruption of Fgf8 causes failure of cell migration in the gastrulating mouse embryo. *Genes Dev.* **13**, 1834-1846.
Sun, X., Mariani, F. V. and Martin, G. R. (2002). Functions of FGF signalling from the apical ectodermal ridge in limb development. *Nature* **418**, 501-508.
Thiery, J. P. (2002). Epithelial-mesenchymal transitions in tumour progression. *Nat. Rev. Cancer* **2**, 442-454.
Trainor, P. A., Tan, S. S. and Tam, P. P. (1994). Cranial paraxial mesoderm: regionalisation of cell fate and impact on craniofacial development in mouse embryos. *Development* **120**, 2397-2408.
Vitelli, F., Taddei, I., Morishima, M., Meyers, E. N., Lindsay, E. A. and Baldini, A. (2002). A genetic link between Tbx1 and fibroblast growth factor signaling. *Development* **129**, 4605-4611.
von Both, I., Silvestri, C., Erdemir, T., Lickert, H., Walls, J. R., Henkelman, R. M., Rossant, J., Harvey, R. P., Attisano, L. and Wrana, J. L. (2004). Foxh1 is essential for development of the anterior heart field. *Dev. Cell* **7**, 331-345.
Waldo, K. L., Kumiski, D. H., Wallis, K. T., Stadt, H. A., Hutson, M. R., Platt, D. H. and Kirby, M. L. (2001). Conotruncal myocardium arises from a secondary heart field. *Development* **128**, 3179-3188.
Washington Smoak, I., Byrd, N. A., Abu-Issa, R., Gooddeeris, M. M., Anderson, R., Morris, J., Yamamura, K., Klingensmith, J. and Meyers, E. N. (2005). Sonic hedgehog is required for cardiac outflow tract and neural crest cell development. *Dev. Biol.* **283**, 357-72.
Xu, H., Morishima, M., Wylie, J. N., Schwartz, R. J., Bruneau, B. G., Lindsay, E. A. and Baldini, A. (2004). Tbx1 has a dual role in the morphogenesis of the cardiac outflow tract. *Development* **131**, 3217-3227.
Yamagishi, H., Maeda, J., Hu, T., McAnally, J., Conway, S. J., Kume, T., Meyers, E. N., Yamagishi, C. and Srivastava, D. (2003). Tbx1 is regulated by tissue-specific forkhead proteins through a common Sonic hedgehog-responsive enhancer. *Genes Dev.* **17**, 269-281.
Yelbuz, T. M., Waldo, K. L., Kumiski, D. H., Stadt, H. A., Wolfe, R. R., Leatherbury, L. and Kirby, M. L. (2002). Shortened outflow tract leads to altered cardiac looping after neural crest ablation. *Circulation* **106**, 504-510.
Zucker, R. M., Hunter, E. S., 3rd and Rogers, J. M. (1999). Apoptosis and morphology in mouse embryos by confocal laser scanning microscopy. *Methods* **18**, 473-480.